Skin Research and Technology 2013; **19**: e27–e36
Printed in Singapore · All rights reserved
doi: 10.1111/j.1600-0846.2011.00603.x

Skin Research and Technology

A Feature-Preserving Hair Removal Algorithm for Dermoscopy Images

Qaisar Abbas[1,2], Irene Fondón Garcia[3], M. Emre Celebi[4] and Waqar Ahmad[1,2]

[1]*Department of Computer Science, National Textile University, Faisalabad, Pakistan* [2]*Center for Biomedical imaging and Bioinformatics, Key Laboratory of Image Processing, Faisalabad, Pakistan* [3]*Department of Signal Theory and Communications, School of Engineering Path of Discovery s/n C. P., Seville, Spain and* [4]*Department of Computer Science, Louisiana State University, Shreveport, Louisiana, USA*

Background/purpose: Accurate segmentation and repair of hair-occluded information from dermoscopy images are challenging tasks for computer-aided detection (CAD) of melanoma. Currently, many hair-restoration algorithms have been developed, but most of these fail to identify hairs accurately and their removal technique is slow and disturbs the lesion's pattern.

Methods: In this article, a novel hair-restoration algorithm is presented, which has a capability to preserve the skin lesion features such as color and texture and able to segment both dark and light hairs. Our algorithm is based on three major steps: the rough hairs are segmented using a matched filtering with first derivative of gaussian (MF-FDOG) with thresholding that generate strong responses for both dark and light hairs, refinement of hairs by morphological edge-based techniques, which are repaired through a fast marching inpainting method. Diagnostic accuracy (DA) and texture-quality measure (TQM) metrics are utilized based on dermatologist-drawn manual hair masks that were used as a ground truth to evaluate the performance of the system.

Results: The hair-restoration algorithm is tested on 100 dermoscopy images. The comparisons have been done among (i) linear interpolation, inpainting by (ii) non-linear partial differential equation (PDE), and (iii) exemplar-based repairing techniques. Among different hair detection and removal techniques, our proposed algorithm obtained the highest value of DA: 93.3% and TQM: 90%.

Conclusion: The experimental results indicate that the proposed algorithm is highly accurate, robust and able to restore hair pixels without damaging the lesion texture. This method is fully automatic and can be easily integrated into a CAD system.

Key words: melanoma – computer-aided detection – dermoscopy – hair segmentation – image inpainting – exemplar-based inpainting – fast marching – derivative of Gaussian

Accepted for publication 20 November 2011

MALIGNANT MELANOMA (MM) is a common malignancy in the US (1) and both invasive and *in-situ* MM has been rapidly increasing cancer in the world. An estimation in 2010 (2), showed that 62,480 incidents and 8420 deaths are counted in the US because of malignant melanoma. It is observed that the MM is a dangerous and deadly type (3) of skin cancer. If MM is detected earlier, then the survival rate of patients is very high (4). For early detection and treatment, a digital dermoscopy device equipped with a computer-aided detection (CAD) system is widely used (5) to analyze skin images, and to aid dermatologists and even practitioners. By using this device, the patterns of skin lesions are clearly visible, which can provide valuable diagnostic information to dermatologists. Moreover, the integration of CAD image processing technique (6) is useful to classify the melanoma-nevus skin lesions. However, the automated classification of melanoma through CAD tool is quite difficult due to hair surrounding the lesions. Therefore, the detection and repair of hair-occluded (7) information of melanoma are often needed. To demonstrate the problem of hairs artifact, the most common melanoma and other pigmented skin lesions (PSLs) are shown in Fig. 1. As shown in this figure, it is very difficult to classify melanoma without removing the hair.

To repair hair pixels from dermoscopy images, researchers are trying to develop image processing based algorithms. However, restoration of melanoma lesions from hair (8) is a

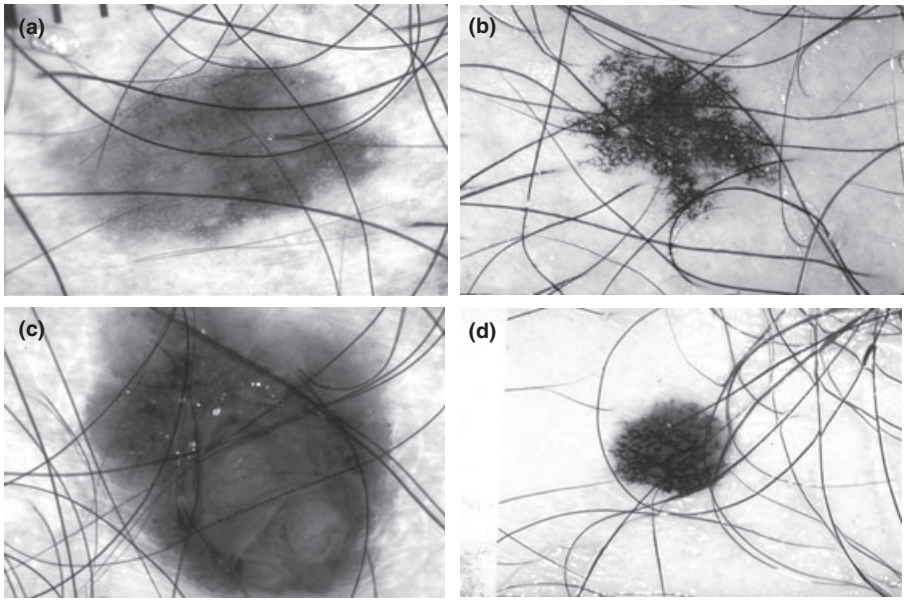

Fig. 1. Problem of hair in different kind of pigmented skin lesions, where (a) Clark Nevus, (b) Lentigo, (c) Melanoma, and (d) Reed Spitz nevus images acquired from digital dermoscopy.

difficult task for automatic CAD system. The task is complicated due to thin, thick hair, same color with lesion and repairing technique often disturbs the texture of melanoma patterns. In the literature, there are a few techniques developed to repair thin and thick hair. In those studies, the algorithms are mainly developed to detect the hair pixels, create undesirable blurring; disturb the texture of the tumor and result in color bleeding. Furthermore, these techniques often require high computational time. The comparative study of the hair-removal algorithm (7) also suggested that the developed techniques are not sufficient, which can be used for further stages of melanoma classification (9, 10) through CAD system. In the literature, there are many algorithms to detect and repair hair pixels, which are shown in Table 1 and briefly described here.

Hairs detection and repair techniques can be generally combined as linear interpolation; Gap search; nonlinear-PDE; exemplar-based, and fast marching inpainting algorithms. An example of linear interpolation hair-removal technique can be found elsewhere (11–13). In the year of 1997, Lee et al. (11) presented the DullRazor hair-removal algorithm that utilized morphological edge-based techniques to identify hair pixels and replaced them by linear interpolation. A similar interpolation method was used by Nguyen et al. (12), but this work involved hair segmentation using morphological edge-based, match filtering and Gaussian curve fitting algorithms. Moreover, in (13), Saugeon et al. used

TABLE 1. Different types of hair-occluded information detection and removal algorithms

Cited Source	Authors	Year	Hair-detection methods	Hair repair methods
(11)	T. K. Lee et al.	1997	Morphological-edge detection	Linear interpolation
(12)	N. H. Nguyen et al.	2010	Morphological-edge detection + Match filtering + Gaussian curve fitting	Linear interpolation
(13)	P.-S .Saugeona et al.	2003	Morphological-edge detection + thresholding	Linear interpolation
(14)	M. G. Fleming et al.	1998	Steger's algorithm + linear searching + discriminate learner	Gap search procedure
(15)	D. H. Chung et al.	2000	Morphological-edge detection	Partial differential equation
(16)	C. A. Z. Barcelos et al.	2009	*NP	Partial differential equation
(17)	F.-Y. Xie et al.	2009	Morphological-edge detection + thresholding	Partial differential equation
(18)	P. Wighton et al.	2008	Morphological-edge detection	Image inpainting
(19)	H. Zhou et al.	2008	Steger's algorithm + 2D-Gaussian partial derivative	Exemplar-based inpainting
(20–22)	Q. Abbas et al.	2010	2D-Derivative of Gaussian	Exemplar-based inpainting
(7, 23)	Q. Abbas et al.	2011	2D-Derivative of Gaussian + morphological-edge detection	Fast marching inpainting

*NP = Not performed.

morphological edge-based and thresholding algorithms for the segmentation of hairs along with the same interpolation method. In these techniques, the thick hairs are effectively segmented, and due to use of interpolation technique to replace the hairs without considering neighborhood patterns of a lesion that are affected by this process. This replacement operation often leads to undesirable blurring and color bleeding. Above all these problems, the weakest point of the technique is it's failure to distinguish between hairs and line segments of the tumor's patterns, disturbing the tumor's texture and therefore making the method unsuitable for dermoscopic images. Different methods were adapted in (14) to detect and repair hair pixels. In that research, Steger's linear searching and discriminate learner techniques are used to detect hairs, which are replaced by Gap search procedure. However, the research is devoted toward detection of hairs rather than their replacement.

A few papers that utilized the concept of nonlinear PDE-based diffusion were also presented in the literature (15–17). For repairing of hairs, the advantage of using nonlinear PDF-based techniques over interpolation is that it is using neighboring information in a natural manner through nonlinear diffusion, filling large gaps while maintaining a sharp boundary. The disadvantage of using this approach is that the diffusion process introduces some blur, which becomes noticeable when filling hair regions. In addition to this problem, this technique has a higher computational than the linear interpolation method. Thus, this technique is a texture-less approach, and is unsuitable for removing hairs from dermoscopy images. In contrast to this approach, there are other algorithms that used image inpainting (18–22) technique to restore hair-occluded information without damaging the texture of lesion. In practice, these inpainting methods are followed to fill missing information by texture synthesis technique. As a result, these methods do not affect the texture part of lesion. The inpainting technique, which combines nonlinear-PDE diffusion and texture synthesis, is called exemplar-based inpainting (19–22). In this type of algorithm, an exceptional consideration is paid toward linear structures. Within these structural elements, the lines abutting the target region only influence the fill order of what is at the core of an exemplar-based texture synthesis algorithm. The result is an algorithm that has the efficiency and qualitative performance of exemplar-based texture synthesis, which also respects the image constraints imposed by the surrounding linear structures. However, the number of iterations and the size of the processing window are required; parameters which are difficult to determine in general. Consequently, the exemplar-based inpainting method does not provide, in practice, an effective solution for hair removal, obtaining less than impressive results.

In contrast with exemplar-based inpainting technique, a fast marching technique was also utilized (7, 23) to repair hairs. In that research, hair removal algorithm is divided into three steps: hairs are detected with the use of a derivative of Gaussian (DOG), refinement by morphological edge-based techniques and then removed by a fast marching image inpainting. The fast marching inpainting algorithm was utilized because it was parameter-less, computational fast and effective as compared with exemplar-based technique. The main advantage of this inpainting algorithm compared to others is that it utilizes an intelligent process to traverse the inpainting domain while (24), transporting the image values in a coherence direction by a structure tensor. In this process, the inpainting technique is switched between diffusion and directional transport by measuring the strength of the coherence. Consequently, this type of fast marching inpainting algorithm is more robust and effective than other methods by adding this 'robust coherence strength'. Therefore, to repair hairs, this inpainting method is followed. Moreover, the detection of hairs is still an issue in the presented algorithms.

In this article, a new hair removal algorithm is presented to repair hair-occluded information from dermoscopy images. To detect effective hairs, first the rough hairs are segmented using a matched filtering with first derivative of gaussian (MF-FDOG) (25) with thresholding that generates strong responses for both dark and light hairs. After that refinements of hairs are performed by morphological edge-based techniques. Finally, repairing step is performed through a fast marching inpainting method. To evaluate the performance of the proposed hair-detection method, statistical diagnostic accuracy

(DA) and texture-quality metric (TQM) measures were utilized. The developed system is tested and compared with the state-of-the-art hair removal algorithm on a set of 100 dermoscopy images, which are obtained as CD resource EDRA-CDROM (26).

Materials and Methods

Dataset

Detecting and repairing of hair-occluded information is tested on a total of 100 dermoscopy images. In this dataset, each image consists of exactly one lesion and there are 70 malignant and 30 Nevus. The dataset was acquired as a CD resource from the two European university hospitals as part of the EDRA-CDROM (26). In this EDRA-CDROM dataset, there are 1064 color dermoscopic images with spatial resolution of 768 × 512 pixels. During routine clinical assessments, all the images in this dataset were captured to imitate a priori probabilities of the diagnosis. From this set of images, 100 dermoscopy images are selected to test the performance of proposed system. The test images are selected on the condition that none of dermoscopy images contained more than 65% hair. In Table 2, the detailed description of the selected dataset is presented. In that dataset, hairs are present almost in every image.

Method

Figure 2 shows the overall diagram of the proposed hair-occluded information repair method that consists of four main stages: color space transforms; rough detection of hairs; refinement of detected hairs, and repairing of hair-occluded information. In this study, all the stages are integrated into a single hair-removal method, which is described in the following paragraphs in detail.

TABLE 2. The detailed description of selected data set that consists of total 100 dermoscopy images of two major categories melanoma and nevus

Sr. No.	lesion types	Total number of lesions	Diameter
1	Melanoma	70	8.10
2	Blue nevus	8	5.9
3	Clark nevus	5	5.0
4	Combined nevus	5	4.1
5	Congenital nevus	5	5.1
6	Dermal nevus	7	3.70

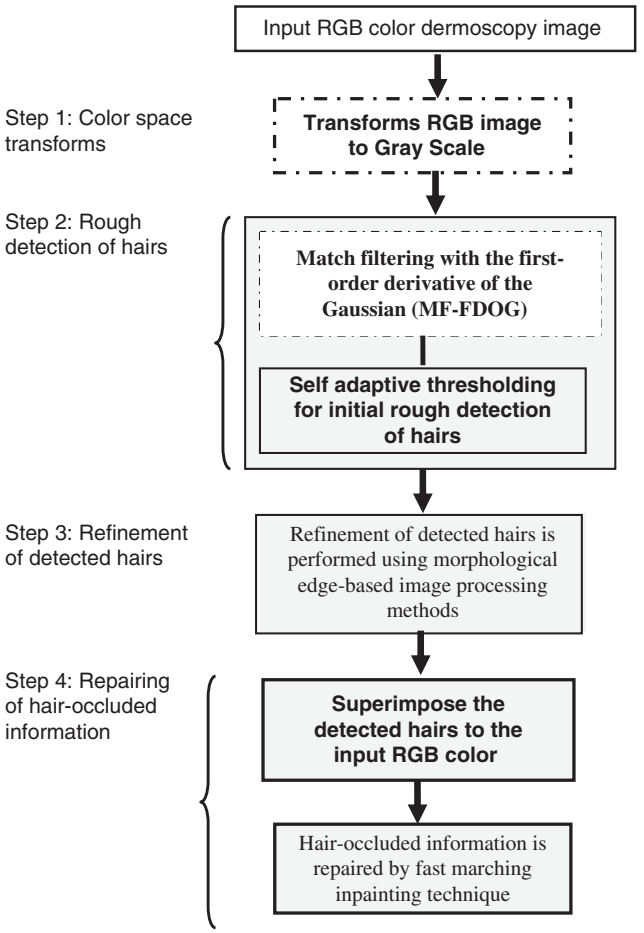

Fig. 2. Flow diagram of the proposed hair-occluded information repair system for dermoscopy images.

Color space transforms

In this article, RGB dermoscopy image is transformed into gray scale image for the detection of hairs-occluded information. However, color transforms (7) are an important step even for the accurate detection of hair pixels from dermoscopy images. It can be noticed that the gray scale is not a perceptually uniform color space. For perceptually uniform color space, CIE $L^*a^*b^*$ and CIE $L^*u^*v^*$ are widely used in the literature. In fact, these two color spaces approximately possess these characteristics, and because of Euclidean distances in those spaces are shown to be approximately correlated with perceptual color differences. In addition to that these color spaces are not capable of considering viewing conditions (27). Therefore, CIECAM02 color appearance model (28) was developed. A color appearance model, CAM, provides us the scene as we would actually see it. Despite these facts about uniformity and view condition, we are using simple gray scale

space because the aim of this article is to develop an effective algorithm for the detection of hairs. However, the others may improve this algorithm by using other color spaces to check the performance. Consequently, the input RGB dermoscopy image is transformed to grayscale, which is visually shown in Fig. 3.

Detection of hair-occluded information

Detection of hair-occluded information from dermoscopy images consists of two major steps. In the first step, the rough hairs are detected using matched filtering with the first-order derivative of the Gaussian (MF-FDOG), which is originally derived from the research (29). In that study, the MF-FDOG technique was effectively developed. Although, the matched filtering with gaussian derivative are detected just hair curve-like objects (25), but there are many tiny objects also segmented in case of dermoscopy images. In addition to that there are some detected hairs, which are not smooth and unbroken. Therefore, we need to refine these detected hairs. In the second step, morphological edge-based techniques are used to refine these detected lines. The integration of morphological edge-based technique to the original MF-FDOG algorithm is due to the fact that hairs are the kind of curves with characteristics: thick as compared with blood vessels in retinopathy images, color of hairs may be very similar to background and hairs can be separated in any direction. Due to these reasons, we are combing morphological edge-based and MF-FDOG techniques to get smooth segmented hairs from dermoscopy images. These two steps are detailed in the subsequent paragraphs.

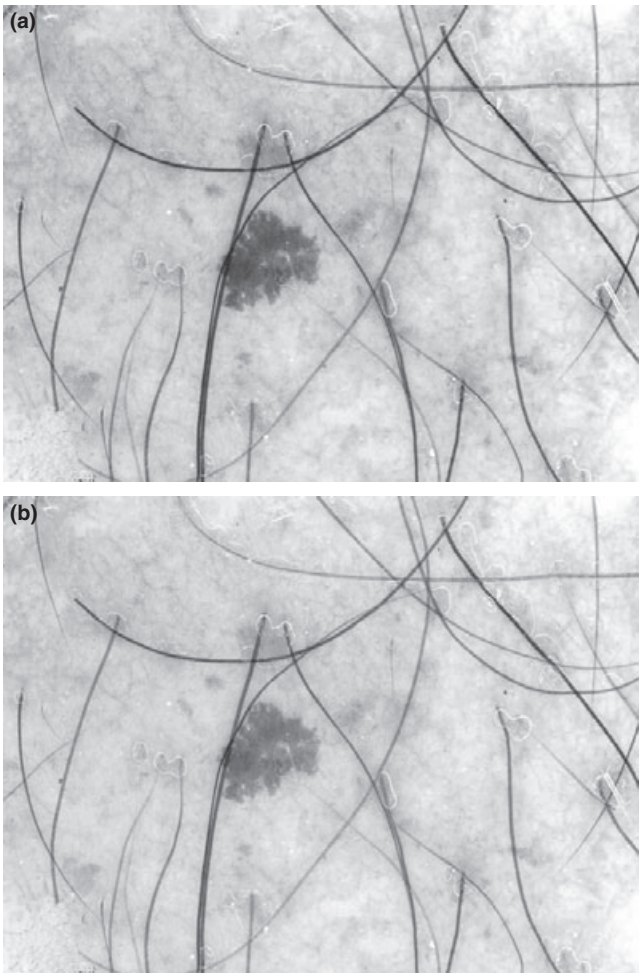

Fig. 3. RGB melanoma image is transformed to gray scale space, where (a) original RGB input image, (b) the transformed image in gray scale.

Rough detection of hairs

Detection of hair-occluded information from dermoscopy images is a challenging task due to several reasons: Hairs have small curvature structure; the color of hairs varies from patient to patient; hairs are thick and thin and the volume of hairs. As a result, the segmentation of hair is a really difficult problem. Specifically, the removal and restoration of hair artifact is an important step prior to subsequent melanoma classification stages.

In this article, for effective segmentation of hairs, the matched filter (MF) with first-order derivative of gaussian (MF-FDOG) (25) is used, which is originally derived from MF (29). The MF-FDOG is defined as:

$$f(x,y) = -\frac{x}{\sqrt{2\pi}s^3}\exp\left(-\frac{x^2}{2s^2}\right), \quad \text{for } |x| \le t.s,\ |y| \le L/2 \tag{1}$$

where s shows the scale of the filter, L is the length of the neighborhood pixels along the y-axis to smooth noise and t is a constant, which is usually set to three because more than 99% (25) of the area under the Gaussian curve lies within three standard deviations. In this first derivative of gaussian equation, the value of L is based on the s parameter. When s is greater, L is set to high, and vice versa. For detection of hairs, the value of t is 4 and L is 6.

These values are determined by experimental experience. To detect hairs in different directions, the $f(x,y)$ is rotated in distinct orientations. The rotation of $f(x,y)$ with angle θ is performed through $f^{\theta}(x',y') = f(x,y)$, where $x' = x\cos\theta + y\sin\theta$ and $y' = y\cos\theta - x\sin\theta$. The first derivative of gaussian can be detected non-hair objects because the original FDOG response, the magnitude around the gaussian is changed quickly . As a result, there is a need to define a criterion to control the FDOG filtering technique.

For this purpose, a thresholding scheme (25) was utilized with MF-FDOG technique to detect hair-occluded information than non-hair objects. The level of threshold T is automatically adjusted by the image's response to FDOG, whereas the value of T is applied to image's response to MF. These two response images, H (by the *MF*) and D (by the *FDOG*) are obtained after filtering the image with the MF-FDOG filters. The local mean image of D is calculated by filtering D with a mean-normalized filter ($\bar{D}_{\mathrm{m}}$), and the value of T is set as $T = (1 + \bar{D}_{\mathrm{m}})c.\mu_H$. Where μ_H the mean value of the response image H, and c is a constant which can be set to 4. The value of c parameter is empirically determined. By applying T to H, the map of hairs is obtained. The initial hairs mask is visually illustrated in Fig. 4(b).

Refinement of detected hairs

Segmented hairs from the previous step are disjoint or weak, unsmooth and unwanted tiny circular objects are also detected. Although, the matched filtering (MF), first derivative of gaussian (FDOG) and thresholding techniques are combined (25) to provide that it can only respond to curve-like objects. However, in case of dermoscopy images, there are some tiny objects, which are also selected such as pigmented network. Therefore, to effectively replace those detected pixels, there is a need to make them stronger, smoother and avoid unwanted nonhair-like objects. To refine this step, morphological edge-based methods are utilized.

Morphological edge-based image-close operation with structuring element (SE) is first performed to fill the larger gaps between lines, and smooth the edges of hair-curves. Using image-close function, the disjoint curves are joined together by filling in the gaps between the curves and by smoothing their outer edges. In this process, a square-shaped SE with a radius of 3 to fill the gaps, and preserve the nature of curve-like objects. This process is repeated until no more change is observed.

After that the connected-component labeling (CC-Labeling) algorithm is performed to extract just curve-like objects as compared with

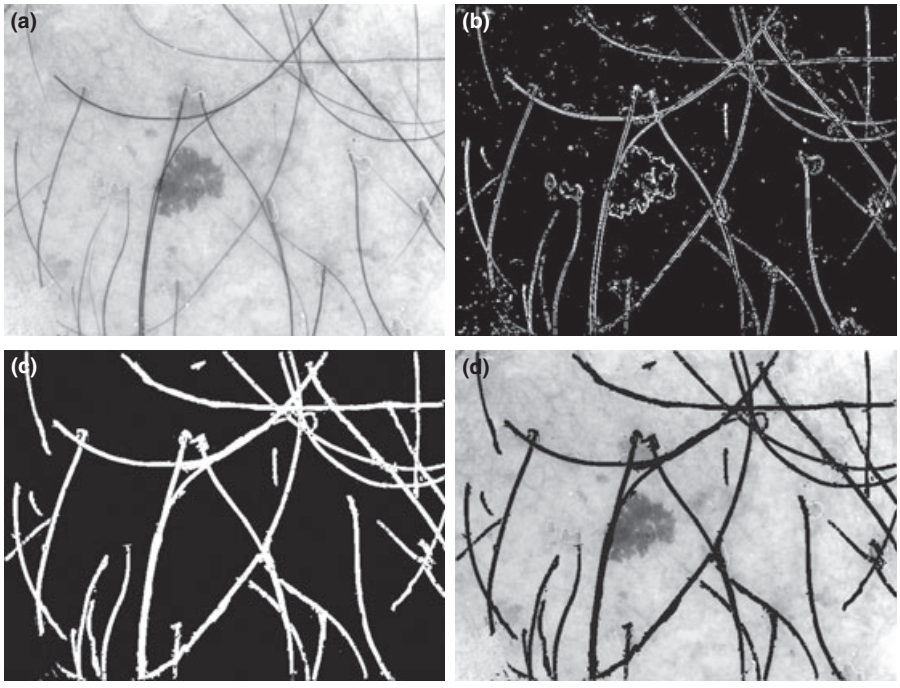

Fig. 4. Result of proposed hairs segmentation algorithm in which, (a) input image in grayscale, (b) detection of rough hairs, (c) refinement of detected hairs, (d) overlaid hairs mask to the original input image.

unwanted tiny or circular objects. To achieve these characteristics, the CC-Labeling algorithm with four-connected objects is performed by imposing the condition of morphological area opening and circularity conditions. The segmented lines or contours can be of the area of skin lesion. Consequently, these two conditions are used to filter unnecessary objects. To impose circularity restriction on CC-Labeling algorithm, a technique developed by Haralick (30) is followed that is based on the mean and variance of the radial distances. Effective hair-occluded curves are segmented using the Haralick circularity condition. At the same time, morphological area opening function is used to filter out small objects, which are smaller than 130 pixels. The value of this condition is empirically determined on this dataset. After second step, the hair-like objects are effectively segmented, and the detection result of hairs is illustrated in Fig. 4(c). Rough detection and refinement of hairs provide a hair mask, which is overlaid onto the original input image in RGB color space using green color [as shown in Fig. 4(d)].

Repairing of hair-occluded information

Restoration and removal of hair in dermoscopy images are performed after the effective detection of hair pixels. For computer-aided diagnosis (CAD) system of melanoma, the hair-like curves must be repaired prior to subsequent stage of classification. To repair lesions from hairs, a fast marching method is utilized, which is developed by Bornemann and Marz (24). Instead of using bilinear interpolation, exemplar-based or non-linear PDF-based inpainting techniques, the fast marching inpainting algorithm is used due to its robustness, parameterless and non-iterative nature. In general, the major objective of using fast marching algorithm is that it can remove the hairs and restore the lesion without affecting the texture part. Therefore, this restoration algorithm has feature-preserving capabilities. There are two studies (7, 23) in the literature, which followed this inpainting method to repair hair pixels. In practice, the basic motivation comes from the fact that it uses a method of rapid progress for inpainting domain through carrying the image of the values in the sense of coherence direction through a robust structure tensor equation. By using this robust structure tensor equation in the inpainting domain (7, 24), this technique measures the strength and switches between diffusion and transport direction. By adding this powerful force consistency, a rapid inpainting method is more effective than other methods, such as exemplar-based inpainting techniques. As a result, this is non-iterative, fast, and reliable method for eliminating noise pixels in dermoscopy images as compared with others. As mentioned above, a fast marching inpainting algorithm is texture-oriented approach compared with others using robust structure tensor equation. The detailed description and numerical stability of this method is not iterative based image inpainting technique and explanation can be found elsewhere (7, 24). Finally, the lesion is restored from the hair-occluded information and this step is visually represented in Fig. 5(c).

Results and Discussion

The feature-preserving hair-occluded information removal algorithm is tested on 100 dermoscopy images, which are obtained as a CD resource from the two European university hospitals as part of the EDRA-CDROM, 2002. In

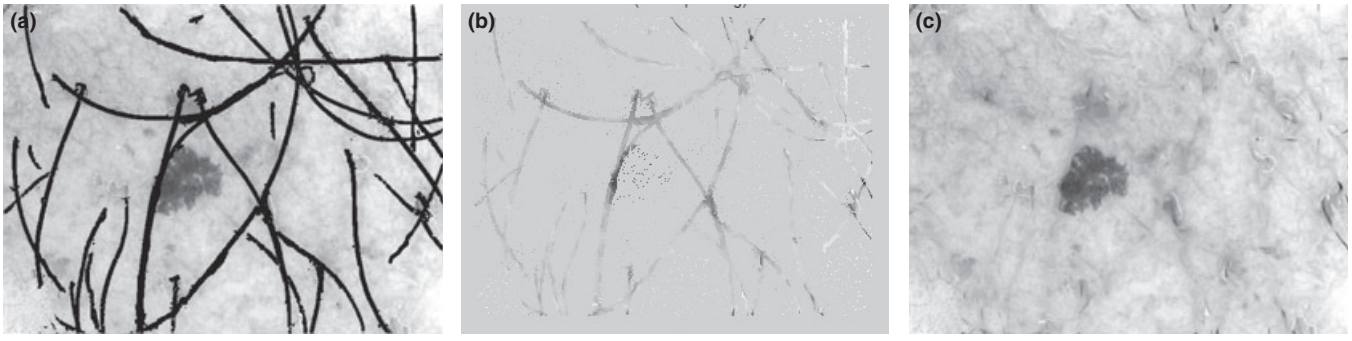

Fig. 5. Example of the hairs-restoration algorithm that shows (a) input figure from Fig. 4(d), (b) detected areas to be repaired from dermoscopy images and (c) hairs removal result.

the selected dataset of 100 images, there are melanoma: 70, blue nevus: 8, clark nevus: 5, combined nevus: 5, congenital nevus: 5, Dermal nevus: 7. The diagnostic accuracy of detection of hairs are tested based on obtained ground truth of hairs mask from an expert dermatologist. All steps of this algorithm are implemented in Matlab 7.6.0.324® (The Mathworks, Natick, MA, USA). All computations were executed on a 2.0 GHz Core to Duo 32-bit Intel processor with 1 GB DDR2 RAM, running Microsoft Windows 7 operating system.

Statistical analysis is performed to determine the accuracy of hair-detection algorithm, which is calculated in terms of true positive (TP); false positive (FP); true negative (TN) and false negative (FN), whereas texture quality measure (TQM) is derived for finding the correctness of hair-removal algorithms. From (TP, FP, TN, FN) values, a diagnostic accuracy (DA) metric is derived based on ground truth contributed by an expert that represents the performance level of the proposed hair-detection algorithm. The value of DA is calculated as:

$$diagnostic\,accuracy\ (DA) = \frac{\mathrm{TP}}{TP + FP + FN} \times 100\% \quad (2)$$

Quantitative and comparison analysis are performed of hairs detection algorithms using this DA metric. To calculate the performance of hair-removal algorithms in terms of features-preserving characteristics, a TQM metric is also calculated based on peak signal to noise ratio (PSNR). A high PSNR value indicates that the restore image is of high quality. The value of PSNR is calculated on each plane of the RGB image that cumulatively describes the image quality as compared with input image. The PSNR value is measured based on window size of 16×16 pixels. It means that each plane image is divided in this window size and then the PSNR is calculated in each window. In addition to this, we have also calculated texture weight of each window by using the co-occurrence matrix. The co-occurrence matrix consists of contrast, correlation, variance and entropy information, which is derived from the gray scale color space. The PSNR and these four-texture weights values are cumulated subtract from the detected hairs pixel values from that area of window size to get significant level of repairing algorithm. Finally, this process is repeated for both original and repair images by performing subtraction operation in these values to get the TQM value. If the value of TQM is high that means the image has feature-preserving capabilities. In this dataset experiments, the value which is greater than 80% is the somewhat acceptable accuracy for the hair removal algorithm.

The DA and TQM metrics are used to compare the performance of proposed detection and removal of hairs algorithm with other three methods: one based on (AbbasEXEMP: 2D-Derivative of Gaussian, Exemplar-based inpainting) (20), other based on (XiePDE: morphological-edge detection + thresholding, PDE-based inpainting) (17), and third one based on (SaugeonLINEAR: morphological-edge detection + thresholding, linear Interpolation) (13). The quantitative results of AbbasEXEMP, XiePDE, SaugeonLINEAR and proposed hair removal algorithm are presented in Table 3.

From Table 3, it can be noticed that the proposed hair removal algorithm achieves high [DA (hair detection: 90.3%) and TQM (hair repair: 90%)] accuracy as compared with XiePDE i.e., [DA (hair detection: 72.5%) and TQM (hair repair: 53.7%)], SaugeonLINEAR i.e., [DA (hair detection: 71%) and TQM (hair repair: 43.1%)] and AbbasEXEMP i.e., [DA(hair detection: 81.2%) and TQM (hair repair: 89%)].

TABLE 3. Comparison of hair-occluded information repairing algorithms for 100 dermoscopy images

Cited Source	Name	Hairs detection methods	Hair-removal methods	*DA	†TQM
(20)	AbbasFAST	2D-Derivative of Gaussian	Exemplar-based inpainting	**81.2%**	**89%**
(17)	XiePDE	Morphological-edge detection + thresholding	PDE-based inpainting	72.5%	53.7%
(13)	SaugeonLINEAR	Morphological-edge detection + thresholding	Linear interpolation	71%	43.1%
		Proposed MF-FDOG + morphological edge-based operations + thresholding	Fast marching inpainting	**90.3%**	**90%**

*DA, diagnostic accuracy for detection of hairs.

†Texture quality measure for repairing of hairs = TQM in percentage.

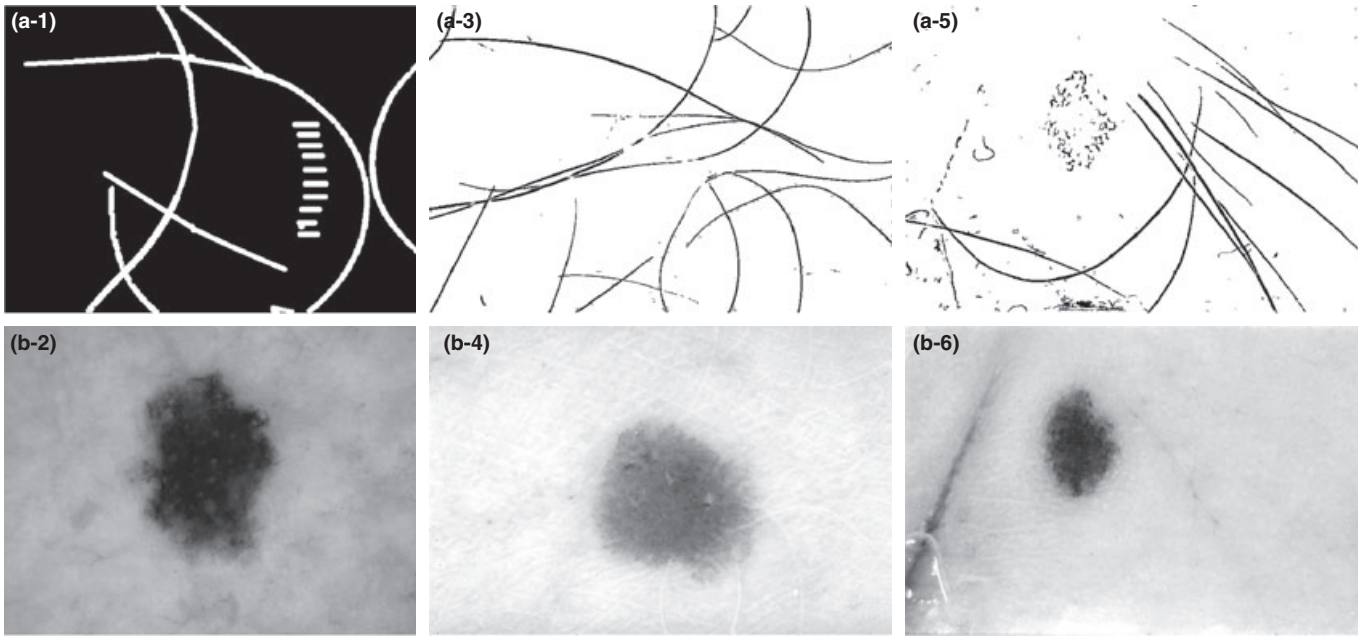

Fig. 6. Examples of the dermoscopy images after performing proposed (a) hairs detection and (b) restoration algorithm.

Among these automated methods, the hair repair performance of the proposed and Abbas-EXEMP methods are almost similar. This is due to the fact that both exemplar-based and fast marching inpainting techniques are texture-oriented approaches compared with others. In contrast with this similar characteristic, a fast marching algorithm is using robust structure tensor equation, and is non-iterative in nature. Therefore, a fast marching algorithm is faster and more effective than exemplar-based algorithms. However, the hair detection diagnostic accuracy of the proposed and AbbasEXEMP algorithms are higher than other techniques. The discrepancy between the proposed algorithm and other techniques (XiePDE, Saugeon-LINEAR) is greater because of the use of effective hair detection and restoration techniques. Some of the example images for both detection of hair-occluded information and removal are shown in Fig. 6. As shown in this figure, our proposed system accurately detects hairs and repairs them without affecting texture part of the lesions.

Conclusion

This article presents a novel algorithm for automatically detecting and repairing of hair-occluded information from dermoscopy images, which has feature-preserving property. The hairs are segmented using MF-FDOG, thresholding, and greatly enhanced through morphological edge-based techniques. After that the hair-occluded information is repaired through the fast marching image inpainting and the lesion is restored without damaging the melanoma texture part. This algorithm was applied to 100 dermoscopy that used hair mask as a ground truth for evaluating the technique. Statistical analysis through diagnostic accuracy (DA) and texture-quality measure (TQM) metrics are used to compare the performance with state-of-the-art techniques. The experimental results indicate that the proposed algorithm is highly accurate, robust and able to restore hairs without damaging melanoma texture part. In this study, the hair-occluded information repair problem is solved by combing the hair segmenting and repairing methods in an unsupervised manner. The approach is highly effective and efficient that can be used to correct diagnosis of melanoma image with hair pixels. For CAD of melanoma, the proposed method can be easily integrated and can be used to increase the performance level.

Acknowledgement

This study was supported by the National Textile University Faisalabad-37610 and higher education commission (HEC) of Pakistan with grant no. 2008GXZ143.

References

1. Rigel DS. Malignant melanoma: perspectives on incidence and its effects on awareness, diagnosis, and treatment. CA Cancer J Clin 1996; 46: 195–198.
2. Jemal A, Siegel R, Xu J, Ward E. Cancer statistics, 2010. CA Cancer J Clin 2010; 60: 277–300.
3. Sneyd MJ, Cox B. Melanoma in Maori, Asian and Pacific peoples in New Zealand. Cancer Epidemiol Biomarkers Prev 2009; 18: 1706–1713.
4. Rigel DS, Carucci JA. Malignant melanoma: prevention, early detection, and treatment in the 21st century. CA Cancer J Clin 2000; 50: 215–236.
5. Argenziano G, Soyer HP, Chimenti S et al. Dermoscopy of pigmented skin lesions: results of a consensus meeting via the internet. J Am Acad Dermatol 2003; 48: 679–693.
6. Johr RH. Dermoscopy: alternative melanocytic algorithms. The ABCD rule of dermatoscopy, menzies scoring method, and 7-point checklist. Clin Dermatol 2002; 20: 240–247.
7. Abbas Q, Celebi ME, García IF. Hair removal methods: a comparative study for dermoscopy images. Biomed Signal Process Control 2011; 6: 395–404.
8. Capdehourata G, Coreza A, Bazzanob A et al. Toward a combined tool to assist dermatologists in melanoma detection from dermoscopic images of pigmented skin lesions. Pattern Recogn 2011; 32: 2187–2196.
9. Iyatomi H, Oka H, Celebi EM, Ogawa K et al. Computer-based classification of dermoscopy images of melanocytic lesions on acral volar skin. J Invest Dermatol 2008; 128: 2049–2054.
10. Serrano C, Acha B. Pattern analysis of dermoscopic images based on Markov random fields. J Pattern Recogn 2009; 42: 1052–1057.
11. Lee TK, Ng V, Gallagher R, Coldman A, McLean D. Dullrazor: a Software approach to hair removal from images. J Comput Biol Med 1997; 27: 533–543.
12. Nguyen NH, Lee TK, Atkinsa MS. Segmentation of light and dark hair in dermoscopic images: a hybrid approach using a universal kernel. In: Dawant BM and Haynor DR, eds. Proc. of SPIE, Medical Imaging: San Diego, CA; 2010: 7623:76234N-8.
13. Saugeon P-S, Guillodb J, Thiran J-P. Towards a computer-aided diagnosis system for pigmented skin lesions. Comput Med Imag Grap 2003; 27: 65–78.
14. Fleming MG, Steger C, Zhang J, Gao J et al. Techniques for a structural analysis of dermatoscopic imagery. Comput Med Imag Grap 1998; 22: 375–389.
15. Chung DH, Sapiro G. Segmentation skin lesions with partial-differential-equation-based image processing algorithms. IEEE T Med Imaging 2000; 19: 763–767.
16. Barcelos CAZ, Pires VB. An automatic based nonlinear diffusion equations scheme for skin lesion segmentation. Appl Math Comput 2009; 215: 251–261.
17. Xie FY, Qin SY, Jiang ZG, Meng RS. PDE-based unsupervised repair of hair-occluded information in dermoscopy images of melanoma. Comput Med Imag Grap 2009; 33: 275–282.
18. Wighton P, Lee TK, Atkinsa MS. Dermoscopic hair disocclusion using inpainting. In: Reinhardt JM and Pluim Josien PW, eds. Proc. of the SPIE medical imaging, San Diego: CA; 2008: 6914:691427–691427-8.
19. Zhou H, Chen M, Gass R, Rehg JM, Ferris L et al. Feature-preserving artifact removal from dermoscopy images. In: Reinhardt JM and Josien PW, eds Proc. of the SPIE medical imaging, San Diego: CA; 2008: 6914:69141B–69141B-9.
20. Abbas Q, Fondon I, Rashid M. Unsupervised skin lesions border detection via two-dimensional image analysis. Comput Methods Program Biomed 2011; 104: e1–e15.
21. Abbas Q, Celebi ME, García IF. Skin tumor area extraction using an improved dynamic programming approach. Skin Res Technol 2012; 18: 133–142.
22. Abbas Q, Celebi ME, García IF. A novel perceptually-oriented approach for skin tumor segmentation. Int J Innov Comput Inform Control 2012; 8: 1–10.
23. Abbas Q, Celebi ME, García IF. Computer-aided pattern classification system for dermoscopy images. Skin Res Technol 2012; 18: 278–289
24. Bornemann F, März T. Fast image inpainting based on coherence transport. J Math Imaging Vis 2007; 28: 259–278.
25. Zhang B, Zhang L, Zhang L, Karray F. Retinal vessel extraction by matched filter with first-order derivative of Gaussian. Comput Biol Med 2010; 40: 438–445.
26. Argeniano G, Soyer PH, De VG, Carli P, Delfino M. Interactive atlas of dermoscopy CD: EDRA medical publishing and New media, 2002.
27. Alman DH, Berns RS, Snyder GD, Larsen WA. Performance testing of color-difference metrics using a color tolerance dataset. Color Res Appl 1989; 14: 139–151.
28. Moroney N, Fairchild M, Hunt R, Li C et al. The CIECAM02 color appearance model. *Proceedings of IS&T/SID 10th color imaging*, Scottsdale, AZ, USA: The society for imaging science and technology; 2002, pp. 23–27.
29. Chaudhuri S, Chatterjee S, Katz N, Nelson M et al. Detection of blood vessels in retinal images using two-dimensional matched filters. IEEE Trans Med Imaging 1989; 8: 263–269.
30. Haralick RM. A measure for circularity of digital figures. IEEE T Syst Man Cybern 1974; SMC-4: 394–396.

Address:
Dr Qaisar Abbas
Assistant Professor/Chairman at
Department of Computer Science,
National Textile University
Faisalabad-37610,
Pakistan
Tel: +92 41 9230081 Ext: 140,
Fax: +92 (41) 9230082
e-mails: drqaisar@ntu.edu.pk and qaisarabbasphd@gmail.com